Metabolic strategies of sharing pioneer bacteria mediating fresh macroalgae breakdown

Maéva Brunet[1], Nolwen Le Duff [1], Tristan Barbeyron[1] and François Thomas[1#]

[1] Sorbonne Université, CNRS, Integrative Biology of Marine Models (LBI2M), Station Biologique de Roscoff (SBR), 29680, Roscoff, France.

Running head: bacterial degradation of fresh macroalgae

#Address correspondence to François Thomas, francois.thomas@sb-roscoff.fr

The authors have no conflict of interest to declare.

Abstract

Macroalgae represent huge amounts of biomass worldwide, largely recycled by marine heterotrophic bacteria. We investigated the strategies of "pioneer" bacteria within the flavobacterial genus *Zobellia* to initiate the degradation of fresh brown macroalgae, which has received little attention compared to the degradation of isolated polysaccharides. *Zobellia galactanivorans* Dsij^T could use macroalgae as a sole carbon source and extensively degrade algal tissues without requiring physical contact, *via* the secretion of extracellular enzymes. This indicated a sharing behaviour, whereby pioneers release public goods that can fuel other bacteria. Comparisons of eight *Zobellia* strains, and strong transcriptomic shifts in *Z. galactanivorans* cells using fresh macroalgae vs. isolated polysaccharides, revealed potential overlooked traits of pioneer bacteria. Besides brown algal polysaccharide degradation, they notably include stress resistance proteins, type IX secretion system proteins and novel uncharacterized Polysaccharide Utilization Loci. Overall, this work highlights the relevance of studying fresh macroalga degradation to fully understand the niche, metabolism and evolution of pioneer degraders, as well as their cooperative interactions within microbial communities, as key players in macroalgal biomass turnover.

Introduction

Macroalgae are major primary producers in coastal zones, acting as a global carbon sink (1). Specific polysaccharides dominate macroalgal extracellular matrices (ECM) and can represent up to 50 % of the dry weight (2). For example, brown algae produce alginates and fucose-containing sulfated polysaccharides (FCSPs). Alginates are linear polymers of β-D-mannuronic (M) and α-L-guluronic acids (G), representing between 10 and 45 % of the algal dry weight (2). FCSPs, accounting for 4-13 % of the dry weight (3), refer to linear or highly

branched polysaccharides containing α-linked L-fucose residues together with a variety of other neutral monosaccharides constituents (galactose, mannose, xylose, rhamnose, etc.) and uronic acids (4). They present many substituents, mainly sulfate and acetyl groups. The structure of brown algal polysaccharides is consequently highly heterogeneous and varies according to species, seasons, geographical locations, thallus part, algal growth stages and environmental factors (3–7). Within the ECM, these carbohydrates are cross-linked and associated with proteins (3-15 %), minerals (7-36 % such as iodine, calcium, iron, copper and magnesium), phenols (1-13 %), vitamins, amino acids and small amounts of lipids (1-5 %) to form a complex matrix (8–11). Besides ECM polysaccharides, brown algae also produce laminarin (β-1,3-glucan) and mannitol (12) as storage carbohydrates.

Marine heterotrophic bacteria are crucial for algal biomass mineralization (13). Macroalgae surfaces are constantly colonized by diverse bacterial communities with densities varying from 10^2 to 10^7cells cm^{-2} of macroalgal tissue (14). A fraction of these communities, mainly *Bacteroidetes*, *Gammaproteobacteria*, *Verrucomicrobia* and *Planctomycetes*, can degrade this complex biomass, showing abilities to hydrolyze purified high molecular weight algal compounds using a considerable enzymatic arsenal (15–18). Over the last 20 years, many studies investigated the algal polysaccharide-processing capabilities of marine heterotrophic bacteria (19), deciphering new catabolic pathways and unraveling the role of carbohydrate active enzymes (CAZymes, http://www.cazy.org, (20)) including glycoside hydrolases (GHs), polysaccharide lyases (PLs) or carbohydrate esterase (CEs), and sulfatases (http://abims.sb-roscoff.fr/sulfatlas/, (21)). In *Bacteroidetes*, CAZymes are usually organized within clusters of coregulated genes involved in carbohydrate binding, hydrolysis and transport, known as Polysaccharide Utilization Loci (PULs). The regulations of these PULs during purified algal substrate degradation were recently studied in a few transcriptome-wide analyses, for both cultivated marine bacteria (22–26) and natural seawater bacterial communities (27). However,

using unique substrates does not reflect the complexity of the responses that might occur during the degradation of intact algal biomass. Considering the algae as a whole could reveal novel genes and catabolic pathways, not induced by soluble purified polysaccharides, but playing key roles in algal biomass recycling in the field. To date information on the mechanisms involved in raw algal material assimilation is scarce. "*Bacillus weihaiensis*" Alg07^T and *Bacillus* sp. SYR4 grow with kelp and red algal powder, respectively (23,28) and *Microbulbifer* CMC-5 grows with thallus pieces of the red alga *Gracilaria corticata* (29). These studies suggested a successive use of the different brown algal polysaccharides contained in the algal ECM (23) and the release of degradation product in the medium (28,29). However, to our knowledge, no previous work investigated the metabolic mechanisms involved in the degradation of fresh macroalgae, hindering our understanding of algal biomass recycling in coastal habitats. Recently, it has been suggested that among bacteria that are able to use soluble algal compounds, only some populations might be specialists for the breakdown of intact macroalgae tissue (19,30,31). This so-called pioneer bacteria would initiate tissue degradation and expose new substrate niches for less efficient community members considered as scavengers.

The genus *Zobellia* (*Flavobacteriaceae* family) is frequently found associated with macroalgae and can account for up to 8 % of natural bacterial communities on decaying algae (32–34). It is composed of 15 validly described strains classified in 8 species (35–38). Their genomes encode numerous CAZymes (263-336 genes representing from 6.4 to 7.6 % of the coding sequences), and sulfatases (39–41). Therefore, *Zobellia* spp. are considered as potent algal polysaccharide degraders. In particular, *Zobellia galactanivorans* Dsij^T, isolated from a red macroalga (35,42), is a model strain to study macroalgal polysaccharide utilization (43). It allowed the discovery of many novel CAZymes and the description of new PULs targeting alginates (44–46), carrageenans (25), agars (47,48), laminarin (49,50), mix-linked glucan (51)

and mannitol (52). Its complete transcriptome analysis revealed common regulations triggered by polysaccharides from the same algal phylum (24). *Z. galactanivorans* Dsij^T is also well equipped to cope with algal defenses and can accumulate iodine (39,53,54). Moreover, a previous study suggested that *Z. galactanivorans* Dsij^T would act as a pioneer bacteria by initiating the breakdown of the kelp *Laminaria digitata,* and demonstrated the crucial role of the alginate lyase AlyA1 in this process (55).

In this study, we aim to better understand the mechanisms controlling fresh macroalgae degradation. To tackle this issue, (i) the complete transcriptome of *Z. galactanivorans* Dsij^T was analyzed during the degradation of three brown macroalgae with distinct chemical composition and compared with purified sugars to decipher key genes and mechanisms specifically triggered on fresh tissues and (ii) the ability of *Z. galactanivorans* to degrade fresh algae tissues was compared with other *Zobellia* spp. to assess its singular behavior and hypothesize on potential genetic determinant in fresh macroalgae breakdown.

Experimental procedure

Purified substrates

Maltose (Sigma-Aldrich, St. Louis, MO, USA), alginate from *Laminaria digitata* (Danisco [ref. Grindsted FD176], Landerneau, France) and FCSPs from *Ascophyllum nodosum* (Algues & Mer [HMWFSA15424, fraction > 100 kDa], Ouessant, France) were tested for growth. Treatment of this commercial FCSP extract with the alginate lyase AlyA1 (45) followed by Carbohydrate-PAGE (56) revealed it contained alginate impurities. Colorimetric assays (57,58) showed that uronic acids accounted for approximately 24 % (w/w) of the FCSP extract. Based on previous measurements of 9 % uronic acid content in pure FCSPs from *A. nodosum* (59), we therefore estimated the alginate contamination in the FCSP extract to be ca.

15%. Alginate, agar (Sigma-Aldrich), kappa- (Goe□mar, St. Malo, France) and iota-carrageenans (Danisco) were used for enzymatic assays.

Strains

Bacterial strains used in this study are listed in **SuppTable1**, together with previous results of their ability to use pure algal compounds (35–37). They were first grown in Zobell 2216 medium (60) at room temperature before inoculation in marine minimum medium (MMM) complemented with antibiotics to which all the tested *Zobellia* strains are resistant (see supplementary methods for composition) and amended with 4 $g.l^{-1}$ maltose as the sole carbon source. Pre-cultures were centrifuged (3200 g, 10 min) and pellets washed twice in 1X saline solution. Cells were inoculated in microcosms at OD_{600} 0.05.

Macroalgae treatment

Healthy *Laminaria digitata*, *Fucus serratus* and *Ascophyllum nodosum* were collected in May 2019 at the Bloscon site (48°43'29.982'' N, 03°58'8.27'' W) in Roscoff (France) and cut in pieces (ca. 2.5-3.5 cm^2) with a sterile scalpel. To clean them from resident epibionts, algal pieces were immersed in 0.1 % Triton in milli-Q water for 10 min followed by 1 % iodine povidone in milli-Q water for 5 min. Finally, algal pieces were rinsed in excess autoclaved seawater for 2 hours, to remove algal exudates and metabolites that could have been produced upon cutting.

Microcosm set up and sampling

All experiments were performed in triplicates, except for *F. serratus* in duplicates, at 20 °C in MMM with macroalgae pieces as the sole carbon source. *Z. galactanivorans* was grown in 50 ml with 10 macroalgal pieces, either young *L. digitata* (<20 cm), *F. serratus* or *A. nodosum*. For comparison it was also grown in the same conditions using 4 $g.l^{-1}$ maltose, alginate or FCSPs. During the exponential phase, culture medium (10 ml) and algal pieces were retrieved

separately on ice for RNA extraction from the free-living and algae-attached bacteria, respectively. On ice, 0.5 volume of killing buffer (20 mM Tris-HCl pH 7.5, 5 mM $MgCl_2$, 20 mM NaN_3) was added to the liquid samples and cell pellets were frozen in liquid nitrogen. Algal pieces were washed twice in killing buffer:H_2O (1:1) and frozen in liquid nitrogen. Samples were stored at -80 °C until RNA extraction. To assess *Z. galactanivorans* growth when cultivated in contact or physically separated from algal tissues, incubations were performed in two-compartment vessels (100 ml each) with round bottom and a 65 mm flat edge opening (Witeg [ref. 0861050], Wertheim, Germany), separated by a 0.2 µm filter. Each compartment was filled with 30 ml of MMM and ten *L. digitata* pieces were immersed in one. For comparative physiology, the eight *Zobellia* strains were grown in 10 ml with three *L. digitata* pieces from the meristem part (< 15 cm from the base).

RNA extraction and sequencing

Details of the protocols are available in Supplementary Methods. Briefly, free-living bacterial cells were lysed by incubation 5 min at 65 °C in lysis buffer (400 µl) and phenol (500 µl). After phenol-chloroform extraction, RNA was treated 1 h at 37 °C with 2 units of Turbo DNAse (ThermoFisher Scientific, Waltham, MA, USA), purified using NucleoSpin RNA Clean-up (Macherey-Nagel, Hoerdt, France) and eluted in 50 µl of nuclease-free water.

RNA from algae-attached bacteria was extracted as follows. Two algal pieces were immersed in killing buffer, vortexed and placed 7 min in an ultrasonic bath to detach bacteria from the algal surface. Algae were removed and cell pellets resuspended in lysis buffer. RNA extraction and DNAse treatment were performed as described above for the free-living bacteria. To avoid RNA loss on purification columns, DNAse was inactivated using the DNAse inactivation reagent (ThermoFisher Scientific).

DNA contamination was checked by PCR with primers S-D-Bact- 0341-b-S-17 and S-D-Bact-0785-a-A-21 targeting the 16S rRNA gene (61). RNA was quantified using the Qubit

RNA HS assay kit (ThermoFisher Scientific) and its integrity assessed on a Bioanalyzer 2100 (Agilent Technology, Santa Clara, CA, USA) with the Agilent RNA 6000 Pico kit.

Paired-end RNA sequencing (RNA-seq) was performed by the I2BC platform (UMR9198, CNRS, Gif-sur-Yvette) on a NextSeq instrument (Illumina, San Diego, CA, USA) using the NextSeq 500/550 High Output Kit v2 (75 cycles) after a Ribo-Zero ribosomal RNA depletion step. A total of 24 samples were sequenced (**SuppTable 2**). Sequencing failed for sample Att_Ldig2 due to poor sample quality.

RNA-seq analysis

Demultiplexed and adapter-trimmed reads were processed with the Galaxy platform (https://galaxy.sb-roscoff.fr). After read quality filtering using Trimmomatic v0.38.0, transcripts were quantified using the pseudo-mapper Salmon v0.8.2 (62) with the *Z. galactanivorans* Dsij^{T} reference genome (retrieved from MicroScope "zobellia_gal_DsiJT_v2"; Refseq NC_015844.1). Raw counts for individual samples were merged into a single expression matrix for downstream analysis. Raw and processed data were deposited under GEO accession number GSE189322. Principal Component Analysis (PCA) and differential abundance analyses were performed on rlog-transformed data using *DESeq2* v1.26.0 package (63) in R v3.6.2 (64). Genes displaying a log2 fold-change |log2FC| > 2 and a Bonferroni-adjusted P-value < 0.05 were considered to be significantly differentially expressed. The upset plot was done using the *ComplexUpset* package (65,66). Hierarchical clustering was performed using the Ward's minimum variance method (67). Graphics were prepared using *ggplot2* (68).

Enzymatic assays

One volume of 0.2 µm filtered supernatant from the microcosms was incubated with 9 volumes of 0.2 % polysaccharide substrate at 28 °C overnight. Controls were prepared with

boiled supernatants. The amount of reducing ends released was quantified using the ferricyanide assay (69). For each sample, the activity measured in controls was subtracted. Finally, the mean value (n=3) measured for the non-inoculated microcosms was subtracted. Significant differences ($P<0.05$) from 0 were tested using t-tests.

CARD-FISH

Algal pieces and culture medium were fixed overnight at 4 °C with 2 % paraformaldehyde. Free-living bacteria were harvested on a 0.2 µm polycarbonate membrane. Catalyzed reporter deposition-fluorescence *in situ* hybridization (CARD-FISH) was performed as described in (34) using the *Zobellia*-specific probe ZOB137 with helpers. Cells on membrane were visualized with a Leica DMi8 epifluorescent microscope (oil objective 63X). Cells on algal tissues were detected with a Leica TCS SP8 confocal microscope (HC PL APO 63X/1.4 oil objective) using the 488 and 638 nm lasers to detect Alexa488 signal and algal autofluorescence signal, respectively. Z-stack images were collected using 1024x1024 scan format (0.29 µm thick layers, 400 Hz scan speed) and visualized using the surface channel mode of the 3D viewer module (Leica Las X software).

Comparative genomics

Zobellia genomes were screened for GHs, PLs, CEs and sulfatases using dbCAN2 (70) on the MicroScope platform (https://mage.genoscope.cns.fr). Homologs (>50 % identity and >80 % alignment) were searched for genes of interest using synteny results on MicroScope.

Results

Zobellia galactanivorans Dsij^T degrades and utilizes fresh brown macroalgae tissues as carbon source

Z. galactanivorans growth was tested with three brown macroalgae from two different orders and with distinct chemical composition, *Laminaria digitata* (order Laminariales), *Fucus serratus* and *Ascophyllum nodosum* (order Fucales), as the sole carbon and energy source. Growth was detected with the three algal species (OD ≈ 0.2-0.5, **Figure 1A**), with tissue bleaching and damages only visible on *L. digitata* pieces after 65 h (**Figure 1B**). *Zobellia*-specific CARD-FISH assays revealed that even if antibiotic-resistant resident epibionts grew in the non-inoculated controls containing *A. nodosum* and *F. serratus* (one replicate), most of the bacterial biomass after 65h in the *Zobellia*-inoculated microcosms was *Zobellia* cells (> 50 %, **SuppFigure 1**).

CARD-FISH assays on *L. digitata* tissues showed gradual tissue colonization by *Z. galactanivorans*, from cell patches at the surface of the *L. digitata* mucilage coat to deeper penetration within the tissue invading the intercellular space (**Figure 1C**).

Transcriptomic shift during fresh macroalgae degradation

Z. galactanivorans Dsij^T transcriptome of free-living cells obtained during macroalgal degradation was compared to the responses occurring with a disaccharide, maltose, and with purified brown algal polysaccharides, alginate and FCSPs. Between 44 and 93 % of the sequenced reads from free-living bacteria grown with macroalgae mapped on the genome of *Z. galactanivorans* Dsij^T (**SuppTable 2**). Multivariate analysis separated samples according to carbon source (**Figure 2A**). Transcriptomes of cells grown with *L. digitata* were closer to that obtained with alginate of FCSPs compared to *A. nodosum* or *F. serratus*.

Differential abundance analysis revealed 1117 and 864 genes up- and down-regulated with at least one substrate, using maltose as control (**SuppTable 3**). Among them, 56 % (628 up-regulated genes) and 52 % (449 down-regulated genes) showed substrate-specific regulations (**Figure 2B)**. In particular, half of the genes regulated with *A. nodosum* and FCSPs were not differentially expressed in any other conditions. *L. digitata* was the algae inducing the highest number of regulations shared with at least one polysaccharide (399, 254 and 217 genes with *L. digitata*, *F. serratus* and *A. nodosum* respectively). More regulations were shared between *L. digitata* and *F. serratus* (116 genes) than *F. serratus* and *A. nodosum* (89 genes) or *L. digitata* and *A. nodosum* (13 genes). Finally, a core set of 70 up-regulated and 59 down-regulated genes responded to the three macroalgae.

Carbohydrate catabolism-related genes

Hierarchical clustering of expression data of the 51 identified PULs in the *Z. galactanivorans* Dsij^{T} genome revealed that PULs predicted to target brown algal polysaccharides grouped together (**Figure 3A**) and were significantly induced with macroalgae. In particular, the alginate-specific PUL29 was significantly overexpressed in all conditions compared with maltose (mean log2FC of 4) and the highest expression was observed with *L. digitata* (**Figure 3B, SuppFigure 2**). Some PULs were exclusively triggered by macroalgae: PUL34 and 35, likely targeting FCSPs (as they encode sulfatases and fucosidases), were significantly triggered by *L. digitata*, PUL4 targeting β-glucan responded to *A. nodosum* and the FCSP PUL3 was induced by both *L. digitata* and *F. serratus*. PUL26 and 27, whose function remains unclear, were both induced by *L. digitata* and FCSPs, as well as by alginate for PUL26 and *F. serratus* for PUL27. Purified FCSPs also induced the expression of 14 PULs outside the described cluster, encompassing a large diversity of targeted substrate (notably β- and α-glucan, sulfated polysaccharides, xylan, unclear substrate). No PUL known to target red algal polysaccharides (e.g. PUL40, 42, 49 or 51) clustered with this set of overexpressed

PULs, suggesting a specific induction of brown algal polysaccharide degradation mechanisms in the presence of brown algal tissues. The measured activity of secreted polysaccharidases corroborates this observation (**Figure 3C**), as only the alginolytic activity was significantly higher when *Z. galactanivorans* was grown on macroalgae compared with the non-inoculated control (t-test, $P<0.05$).

On the other hand, PULs targeting simple sugars (maltose and fructose) or polysaccharides absent from brown algae (starch and chitin) were repressed with macroalgae and purified polysaccharides (**Figure 3A**). The starch PUL12 was strongly underexpressed in all conditions while the chitin PUL31 showed a significant repression only with algal polysaccharides.

Specific induction with fresh algal tissues

To unravel pathways specifically governing the degradation of fresh macroalgal biomass, we further focused on genes upregulated with at least one macroalgal species compared to maltose and purified polysaccharides. We detected 41, 59 and 189 genes following this pattern with *L. digitata*, *F. serratus* or *A. nodosum*, respectively (**SuppTable 4**). It included few CAZyme-encoding genes (**Figure 4**), notably two genes within putative FCSP PULs (*zgal_205* [GH117 in PUL3] and *zgal_3445* [GH88 in PUL34]). Other polysaccharidase genes outside classical PUL structures were induced with *A. nodosum*, such as *alyA1* (*zgal_1182*, alginate lyase PL7), *cgaA* (*zgal_3886*, glucan 1,4-α-glucosidase GH15), *agaC* (*zgal_4267*, β-agarase GH16), *pelA1* (*zgal_3770*, pectate lyase PL1) and *dssA* (*zgal_3183*, sheath polysaccharide lyase PL9). GT2 (*zgal_2991*, *4154*) and GT4 (*zgal_2990*, *3759*) were also triggered with macroalgae. Additionally, many genes linked to oxidative stress responses and Type IX secretion systems (T9SS) were specifically induced with macroalgae (**Figure 4**). A large gene cluster (*zgal_1071-1105)* notably encoding three oxidoreductases, a DNA topoisomerase and a peroxiredoxin was up-regulated with *L. digitata* and *F. serratus*. Other

genes encoding antioxidant proteins were triggered, especially on *L. digitata*, such as the superoxide dismutase SodC (ZGAL_114) or a β-carotene hydroxylase (ZGAL_2972), as well as a carboxymuconolactone decarboxylase family protein (ZGAL_1598) which includes enzyme involved in antioxidant defense (71). Two catalases (ZGAL_1427 and ZGAL_3559) were induced in the presence of *L. digitata* and *F. serratus* in comparison to maltose and alginate (**SuppTable4**). Several genes predicted to encode T9SS components were significantly induced during macroalga degradation, in particular with *A. nodosum* (14 out of 33 genes identified in the genome, against 1 and 5 with *L. digitata* and *F. serratus* respectively) (**Figure 4**). They include particularly genes encoding SprF family proteins and T9SS-associated PG1058-like proteins. In addition, 7 unknown proteins containing a conserved C-terminal domain (CTD) from families TIGR04131 (gliding motility - ZGAL_2022, 2761, 2762, 3727) and TIGR04183 (Por secretion system - ZGAL_93, 1124, 4310) were triggered. These CTDs are typical of cargo proteins secreted by the T9SS.

Effect of bacterial attachment to macroalgae

Transcriptomes of algae-attached cells were compared to that of free-living bacteria. To minimize bias due to poor sequencing depth (caused by a high proportion of eukaryotic rRNA in algae-attached samples [**SuppTable 2**]), we discarded samples from *A. nodosum* microcosms (up to 70 % of uncovered coding regions) and only considered upregulated genes (not the down-regulated ones) in attached versus free-living bacteria. Respectively 19 and 14 genes were significantly induced in bacteria attached to *L. digitata* or *F. serratus* (**Figure 5A**), including a shared set of 5 genes from a genomic region (*zgal_4237-4246*) putatively involved in stress responses. Attachment to *L. digitata* induced the expression of two TetR-type transcriptional regulators, 2 YceI family proteins which might be involved in oxidative stress response via isoprenoide synthesis (72,73) and 5 chaperones (**Figure 5A**). Cells

attached to *F. serratus* notably overexpressed 2 TonB-dependent receptors not associated with a SusD-like protein, likely not involved in carbohydrate metabolism.

To assess if algal degradation requires biofilm formation, *Z. galactanivorans* was grown either in contact or physically separated from algal pieces (**Figure 5B**). After 6 days, algal tissues were visually starting to decompose when bacteria were separated from algae, although to a lesser extent compared to the "contact" condition. Furthermore, extracellular alginolytic activity increased even without physical bacteria/algae contact and reached similar levels to that observed in the "contact" condition after 90 h.

Comparative physiology and genomics of fresh macroalga degradation by *Zobellia*

The degrading abilities of other members of the genus *Zobellia* were investigated (**Figure 6A**). All tested *Zobellia* strains used fresh *L. digitata* tissues for their growth. *Z. galactanivorans* Dsij^T had the highest final cell density (OD_{600} = 1.5) and shortest generation time (5.09 h). *Z. nedashkovskayae* Asnod3-E08-A formed cell aggregates that biased OD_{600} readings, likely explaining the apparent limited growth (final OD_{600} = 0.4) and long generation time (t_{gen} = 16.33 h). Other strains showed intermediate behaviors ($OD_{600} \approx 1$, 5.92 < t_{gen} < 11.74 h). These growth differences were reflected in the final aspect of macroalgal pieces. Only *Z. galactanivorans* Dsij^T completely broke down algal tissues after 91 h. Both *Z. nedashkovskayae* strains caused limited algal peeling and breakdown at the corners of the pieces., No visible trace of degradation was detected for other strains. A strong negative correlation was found between the number of GHs and the generation time (Spearman, rho = -0.90; P = 0.006) (**Figure 6A**, **SuppTable 5**). Twenty-two out of the 305 genes up-regulated by *Z. galactanivorans* Dsij^T with *L. digitata* compared to maltose had no homologs in the genome of the seven other *Zobellia* strains (**SuppTable 6**). They include two GHs, *zgal_3349*

(GH20 in PUL33) and *zgal_3470* (GHnc in PUL35), and a susCD-like pair (*zgal_3440*, *3441*) in PUL34. Other up-regulated genes within the FCSP PUL34/35 are not conserved in all *Zobellia* strains (**Figure 6B**). Likewise, several alginolytic genes were not conserved across the genus, especially in the two *Z. roscoffensis* strains that lack 7 of them. *zgal_1182* and *zgal_4327*, encoding the extracellular endo-alginate lyases AlyA1 and AlyA7 respectively, were not conserved in the other strains (*zgal_4327*) or only found in the *Z. nedashkovskayae* strains (*zgal_1182*). Two other genes related to carbohydrate assimilation (*zgal_334* and *zgal_2296* encoding a GHnc and a lipoprotein with CBM22, respectively) are missing in five strains (**SuppTable 6**). *zgal_334* neighbors genes encoding sulfatases, fucosidases and PLs and might belong to a FCSP-targeting cluster (absent from the 51 identified PULs as the pair *susCD*-like is absent).

Discussion

Zobellia galactanivorans Dsij^T acts as a sharing pioneer in brown macroalgae degradation

By degrading macroalgae, marine heterotrophic bacteria are central to nutrient cycling in coastal habitats. The ecological strategies of different functional guilds not equally equipped to process biomass were recently conceptualized (19,30,31). First, pioneer bacteria degrade complex organic matter by producing specific hydrolytic enzymes. The hydrolysate can then fuel other bacteria called exploiters or scavengers, which cannot feed on intact substrates. Such cooperative interactions were previously characterized during alginate (74) or chitin (75,76) assimilation. Hence, in nature pioneer bacteria likely control the initial attack on fresh macroalgae, a hitherto rarely studied process that cannot be fully deciphered when using purified polysaccharides or crushed algae. Here, we showed that *Z. galactanivorans* Dsij^T uses healthy brown algal tissues for its growth, highlighting its pioneer role in algal biomass

recycling. Similar growth rates were observed with three brown algal species, and *Z. galactanivorans* completely broke down *L. digitata* tissues. Transcriptomes obtained with *L. digitata* were closest to that with alginate and FCSP, suggesting a greater capacity to access and digest ECM polysaccharides within the *L. digitata* tissues compared to *A. nodosum* and *F. serratus*. The limited degradation of Fucales tissues might originate from their higher phlorotannin content (77), possibly inhibiting CAZymes (78). In addition, *A. nodosum* induced a wider cellular response with many specific regulations. This might partly be due to the growth of antibiotic-resistant epiphytic bacteria that could have affected *Z. galactanivorans* behavior or to its much thicker and rigid thallus. Furthermore, *A. nodosum* is associated with various symbionts, especially the obligate endophytic fungus *Mycophycias ascophylli* (79) that secretes compounds potentially preventing tissue grazing and/or offering new substrate niches.

We showed that although *Z. galactanivorans* can colonize *L. digitata*, it does not require a physical contact to initiate degradation. Furthermore, only few upregulated genes were detected in surface-attached vs. free-living cells. While difficulties to extract RNA from algae-attached bacteria resulted in poor sequencing coverage, it should still have been possible to detect strong upregulations in attached cells. Overall, our results indicate that surface attachment is not required for the utilization of algal biomass by *Z. galactanivorans* Dsij^{T}. This suggests a crucial role for secreted enzymes to initiate degradation, in line with the measured extracellular alginolytic activity. Constitutively expressed extracellular enzymes, such as the alginate lyases AlyA1 and AlyA7 (44), would rapidly release diffusible degradation products, allowing remote substrate sensing. We previously showed that *Z. galactanivorans* accumulates low molecular weight (LMW) alginate oligosaccharides when grown with purified alginate and algal tissues (44,55). Our results therefore confirms that *Z. galactanivorans* would be a “sharing” pioneer providing degradation products as public goods

to other taxa (55), contrary to "selfish" pioneers which sequester LMW products by producing essentially surface-associated hydrolytic enzymes with minor loss of hydrolysate to the medium (80,81).

We further evidenced that this pioneer behavior can be strain-specific within the alga-associated genus *Zobellia*. All *Zobellia* spp. tested successfully grew with fresh *L. digitata* but without causing pronounced tissues damages as observed with *Z. galactanivorans*. Their catabolic profiles (**SuppTable 1**) indicate different growth capacities with purified brown algal sugars. For example, *Z. roscoffensis* strains and *Z. laminariae* KMM 3676^T display limited or no abilities to use alginate, FCSPs and laminarin for their growth. Hence, with macroalgae, they likely did not use these complex polysaccharides but rather fed on soluble algal exudates (e.g. mannitol). Comparative genomics suggested that CAZyme content influences the strain capacity to use and break down fresh algal tissues. In particular, some strains lack homologs of overexpressed genes contained in *L. digitata*-induced PULs targeting alginate or FCSPs. For example, *alyA1* homologs were only found in the two other strains that caused visible algal damage (*Z. nedashkovskayae* Asnod2-B07-B^T and Asnod3-E08-A). Accordingly, *alyA1* is known to have a crucial role in initiating algae breakdown (55). Such genes would therefore represent potential genetic determinants of pioneer bacteria.

Deciphering the metabolic mechanisms involved in fresh tissue breakdown, including new catabolic pathways

Regardless of the algal species, the well-characterized alginolytic PUL29 was the most induced among all PULs. Alginate is the most abundant polysaccharide in brown algal ECM and likely the most accessible as it embeds the cellulose-FCSP network (11). This PUL was particularly triggered with *L. digitata*, likely reflecting the higher alginate content in this species (2) and/or an easier substrate accessibility. Furthermore, several uncharacterized PULs were triggered with macroalgae. Three out of the seven predicted FCSP PULs were

399 significantly upregulated with macroalgae but not with extracted *A. nodosum* FCSPs, and to
400 various degrees depending on algal species. In addition, two PULs with unclear function
401 (PUL26 and 27) were induced with both FCSPs and macroalgae. This suggests different
402 substrate specificities, consistent with the large structural diversity of FCSPs and cross-
403 linkage to other compounds (4,7,82) which might not be equally extracted during purification.
404 By preserving the original polysaccharide structure and environment, the study of fresh
405 macroalga degradation may therefore be a more effective way to reveal specific genes crucial
406 for macroalgae breakdown by pioneer bacteria but undetectable when using purified
407 polysaccharides.
408 By contrast to alginate- and FCSP-targeting PULs, the characterized laminarin PUL11 and
409 PUL28 were poorly regulated with the three algae. An uncharacterized β-glucan PUL4 was
410 significantly induced only with *A. nodosum*, and also found triggered with purified laminarin
411 in a previous study (24). As raised above, the presence of endosymbionts in *A. nodosum* could
412 result in specific laminarin structures that might be targeted by PUL4. The absence of
413 induction of typical laminarin PULs with macroalgae might also indicate that *Z.*
414 *galactanivorans* Dsij^{T} first uses ECM polysaccharides and later access intracellular storage
415 polysaccharides. Such a prioritization of multiple substrates within algal material was
416 previously observed for *Bacillus weihaiensis* Alg07^{T} grown on algal powder (23). Koch *et al.*
417 (26) showed that *Alteromonas macleodii* 83-1 prioritized laminarin over alginate and pectin
418 when grown on a mixture of purified polysaccharides. Thus, prioritization might differ
419 between bacterial strains and whether substrates are under soluble form or within algal tissues,
420 underlining the importance to consider intact macroalgae to understand the pioneer behavior.
421 Furthermore, future time-resolved transcriptome analyses could inform on regulations at
422 different degradation stages and help decipher prioritization effects.

Besides carbohydrate utilization, our approach unveiled several traits specifically induced upon macroalgal degradation and potentially linked to the pioneer behavior, including the resistance to algal defense and T9SS. One of the algal defense mechanisms is the production of reactive oxygen species (ROS), which in *L. digitata* is partly induced by endogenous elicitors (i.e. oligo-alginates) derived from the degradation of their own cell wall (83). Breakdown of *L. digitata* tissues by *Z. galactanivorans* likely produced large amounts of elicitors and consequently triggered a massive oxidative burst, in line with the strong induction of genes encoding ROS-detoxifying enzymes in this condition. In contrast, *A. nodosum* and *F. serratus* do not respond to the addition of endogenous elicitors (84), potentially explaining the lower induction of antioxidant pathways in *Z. galactanivorans* Dsij^{T} with these algae. Another algal defense response is the emission of halogenated compounds. One vanadium-dependent iodoperoxidase (vIPO3) and a haloacid dehalogenase (HAD, (54)) were significantly up-regulated with *A. nodosum* compared with alginate and maltose respectively. HAD expression was also 3-fold higher with *L. digitata* and *F. serratus* compared to maltose, although large variations precluded significance. The induction of stress resistance mechanisms was even more pronounced in bacteria attached to *L. digitata* tissues through the expression of chaperones. Overall, our results suggest that pioneer bacteria might have evolved to cope with increasing stress levels upon algal degradation. By metabolizing toxic compounds, they might favor the growth of less stress-resistant scavenger bacteria, a hitherto overlooked additional benefit besides the opening of new substrate niches.

Specific to *Bacteroidetes*, T9SS is involved in biofilm formation, protease virulence factors delivery and secretion of polysaccharidases and cell-surface gliding motility adhesins (85,86). Here, we showed that growth with macroalgae strongly induced genes encoding T9SS components, T9SS-translocated proteins and several glycosyl transferases from families GT2 and GT4. Glycosyltransferases with a GT4_CapM-like domain were recently shown to N-

glycosylate CTD in *Cytophaga hutchinsonii*, an essential step for the recognition of cargo proteins by T9SS (87). Hence, our data suggest T9SS might be a key determinant of pioneer behavior in the *Bacteroidetes* phylum, to secrete ECM-targeting CAZymes and/or attach to macroalgal surfaces.

Conclusion

This study provides the first insights into the metabolic strategies of sharing pioneer bacteria during fresh macroalgae utilization and represents a source of potential genetic determinants for further functional characterization. Altogether, our results raised the relevance to consider the whole complexity of macroalgae tissues in further degradation studies, as it would take a step forward in the understanding of the algal biomass recycling through the identification of new metabolic pathways or the characterization of bacterial cooperative interactions.

Acknowledgments

The authors thank Tatiana Rochat for advice during transcriptomic analyses, Sébastien Colin for guidance in confocal manipulation, Philippe Potin and Cécile Hervé for helpful discussions and Yan Jaszczyszyn from the I2BC sequencing platform. This work has benefited from the facilities of the Genomer platform and from the computational resources of the ABiMS bioinformatics platform (FR 2424, CNRS-Sorbonne Université, Roscoff), which are part of the Biogenouest core facility network. This work was funded by the French Government via the National Research Agency programs ALGAVOR (ANR-18-CE02-0001-01) and IDEALG (ANR-10-BTBR-04).

Competing interests

The authors have no conflict of interest to declare.

Author contributions (according to CRediT taxonomy)

Conceptualization: MB, TB and FT. Data curation: MB, FT. Formal analysis: MB, FT. Funding acquisition: FT. Investigation: all authors. Supervision: TB, FT. Visualization: MB. Writing original draft: MB. Writing review and editing: MB, TB and FT.

References

1. Duarte C, Middelburg JJ, Caraco N. Major role of marine vegetation on the oceanic carbon cycle. Biogeosciences. 2005;2:1–8.

2. Kloareg B, Quatrano RS. Structure of the cell walls of marine algae and ecophysiological functions of the matrix polysaccharides. Ocean Mar Biol Annu Rev. 1988;26:259–315.

3. Fletcher HR, Biller P, Ross AB, Adams JMM. The seasonal variation of fucoidan within three species of brown macroalgae. Algal Res. 2017;22:79–86.

4. Deniaud-Bouët E, Hardouin K, Potin P, Kloareg B, Hervé C. A review about brown algal cell walls and fucose-containing sulfated polysaccharides: Cell wall context, biomedical properties and key research challenges. Carbohydr Polym. 2017;175:395–408.

5. Haug A, Larsen B, Smidsrød O. Uronic acid sequence in alginate from different sources. Carbohydr Res. 1974;32(2):217–25.

6. Bruhn A, Janicek T, Manns D, Nielsen MM, Balsby TJS, Meyer AS, et al. Crude

fucoidan content in two North Atlantic kelp species, *Saccharina latissima* and *Laminaria digitata*—seasonal variation and impact of environmental factors. J Appl Phycol. 2017;29(6):3121–37.

7. Ponce NMA, Stortz CA. A comprehensive and comparative analysis of the fucoidan compositional data across the Phaeophyceae. Front Plant Sci. 2020;11:556312.

8. Fleurence J. The enzymatic degradation of algal cell walls: A useful approach for improving protein accessibility? J Appl Phycol. 1999;11(3):313–4.

9. Verhaeghe EF, Fraysse A, Guerquin-Kern JL, Wu T Di, Devès G, Mioskowski C, et al. Microchemical imaging of iodine distribution in the brown alga *Laminaria digitata* suggests a new mechanism for its accumulation. J Biol Inorg Chem. 2008;13(2):257–69.

10. Schiener P, Black KD, Stanley MS, Green DH. The seasonal variation in the chemical composition of the kelp species *Laminaria digitata*, *Laminaria hyperborea*, *Saccharina latissima* and *Alaria esculenta*. J Appl Phycol. 2015;27(1):363–73.

11. Deniaud-Bouët E, Kervarec N, Michel G, Tonon T, Kloareg B, Hervé C. Chemical and enzymatic fractionation of cell walls from Fucales: Insights into the structure of the extracellular matrix of brown algae. Ann Bot. 2014;114(6):1203–16.

12. Michel G, Tonon T, Scornet D, Cock JM, Kloareg B. Central and storage carbon metabolism of the brown alga *Ectocarpus siliculosus*: Insights into the origin and evolution of storage carbohydrates in Eukaryotes. New Phytol. 2010;188(1):67–81.

13. Mann K. Ecology of coastal waters - A systems approach, Berkeley: University of California Press. 1982.

513 14. Egan S, Harder T, Burke C, Steinberg P, Kjelleberg S, Thomas T. The seaweed
514 holobiont: Understanding seaweed-bacteria interactions. FEMS Microbiol Rev.
515 2013;37(3):462–76.

516 15. Kirchman DL. The ecology of *Cytophaga-Flavobacteria* in aquatic environments.
517 FEMS Microbiol Ecol. 2002;39(2):91–100.

518 16. Thomas F, Hehemann JH, Rebuffet E, Czjzek M, Michel G. Environmental and gut
519 *Bacteroidetes*: The food connection. Front Microbiol. 2011;2:93.

520 17. Teeling H, Fuchs BM, Becher D, Klockow C, Gardebrecht A, Bennke CM, et al.
521 Substrate-controlled succession of marine bacterioplankton populations induced by a
522 phytoplankton bloom. Science (80-). 2012;336(6081):608–11.

523 18. Wietz M, Wemheuer B, Simon H, Giebel HA, Seibt MA, Daniel R, et al. Bacterial
524 community dynamics during polysaccharide degradation at contrasting sites in the
525 Southern and Atlantic Oceans. Environ Microbiol. 2015;17(10):3822–31.

526 19. Arnosti C, Wietz M, Brinkhoff T, Hehemann J-H, Probant D, Zeugner L, et al. The
527 biogeochemistry of marine polysaccharides: sources, inventories, and bacterial drivers
528 of the carbohydrate cycle. Ann Rev Mar Sci. 2020;13:9.1-9.28.

529 20. Lombard V, Golaconda Ramulu H, Drula E, Coutinho PM, Henrissat B. The
530 carbohydrate-active enzymes database (CAZy) in 2013. Nucleic Acids Res.
531 2014;42(D1):490–5.

532 21. Barbeyron T, Brillet-Guéguen L, Carré W, Carrière C, Caron C, Czjzek M, et al.
533 Matching the diversity of sulfated biomolecules: Creation of a classification database
534 for sulfatases reflecting their substrate specificity. PLoS One. 2016;11(10):1–33.

22. Tang K, Lin Y, Han Y, Jiao N. Characterization of potential polysaccharide utilization systems in the marine *Bacteroidetes Gramella flava* JLT2011 using a multi-omics approach. Front Microbiol. 2017;8:220.

23. Zhu Y, Chen P, Bao Y, Men Y, Zeng Y, Yang J, et al. Complete genome sequence and transcriptomic analysis of a novel marine strain *Bacillus weihaiensis* reveals the mechanism of brown algae degradation. Sci Rep. 2016;6:38248.

24. Thomas F, Bordron P, Eveillard D, Michel G. Gene expression analysis of *Zobellia galactanivorans* during the degradation of algal polysaccharides reveals both substrate-specific and shared transcriptome-wide responses. Front Microbiol. 2017;8:1808.

25. Ficko-Blean E, Préchoux A, Thomas F, Rochat T, Larocque R, Zhu Y, et al. Carrageenan catabolism is encoded by a complex regulon in marine heterotrophic bacteria. Nat Commun. 2017;8:1685.

26. Koch H, Dürwald A, Schweder T, Noriega-Ortega B, Vidal-Melgosa S, Hehemann JH, et al. Biphasic cellular adaptations and ecological implications of *Alteromonas macleodii* degrading a mixture of algal polysaccharides. ISME J. 2019;13(1):92–103.

27. Bunse C, Koch H, Breider S, Simon M, Wietz M. Sweet spheres: succession and CAZyme expression of marine bacterial communities colonizing a mix of alginate and pectin particles. Environ Microbiol. 2021;23(6):3130–48.

28. Kang S, Kim JK yu. Reuse of red seaweed waste by a novel bacterium, *Bacillus* sp. SYR4 isolated from a sandbar. World J Microbiol Biotechnol. 2015;31:209–17.

29. Jonnadula R, Verma P, Shouche YS, Ghadi SC. Characterization of *Microbulbifer* strain CMC-5, a new biochemical variant of *Microbulbifer elongatus* type strain DSM6810^T isolated from decomposing seaweeds. Curr Microbiol. 2009;59:600–7.

30. Hehemann JH, Arevalo P, Datta MS, Yu X, Corzett CH, Henschel A, et al. Adaptive radiation by waves of gene transfer leads to fine-scale resource partitioning in marine microbes. Nat Commun. 2016;7:12860.

31. Gralka M, Szabo R, Stocker R, Cordero OX. Trophic interactions and the drivers of microbial community assembly. Curr Biol. 2020;30(19):R1176–88.

32. Martin M, Barbeyron T, Martin R, Portetelle D, Michel G, Vandenbol M. The cultivable surface microbiota of the brown alga *Ascophyllum nodosum* is enriched in macroalgal-polysaccharide-degrading bacteria. Front Microbiol. 2015;6:1487.

33. Dogs M, Wemheuer B, Wolter L, Bergen N, Daniel R, Simon M, et al. *Rhodobacteraceae* on the marine brown alga *Fucus spiralis* are abundant and show physiological adaptation to an epiphytic lifestyle. Syst Appl Microbiol. 2017;40(6):370–82.

34. Brunet M, Le Duff N, Fuchs B, Amann R, Barbeyron T, Thomas F. Specific detection and quantification of the marine flavobacterial genus *Zobellia* on macroalgae using novel qPCR and CARD-FISH assays. Syst Appl Microbiol. 2021;44(6):126269.

35. Barbeyron T, L'Haridon S, Corre E, Kloareg B, Potin P. *Zobellia galactanovorans* gen. nov., sp. nov., a marine species of *Flavobacteriaceae* isolated from a red alga, and classification of [*Cytophaga*] *uliginosa* (ZoBell and Upham 1944) Reichenbach 1989 as *Zobellia uliginosa* gen. nov., comb. nov. Int J Syst Evol Microbiol. 2001;51(3):985–97.

36. Barbeyron T, Thiébaud M, Le Duff N, Martin M, Corre E, Tanguy G, et al. *Zobellia roscoffensis* sp. nov. and *Zobellia nedashkovskayae* sp. nov., two flavobacteria from the epiphytic microbiota of the brown alga *Ascophyllum nodosum*, and emended

description of the genus *Zobellia*. Int J Syst Evol Microbiol. 2021;71(8).

37. Nedashkovskaya OI, Suzuki M, Vancanneyt M, Cleenwerck I, Lysenko AM, Mikhailov V V., et al. *Zobellia amurskyensis* sp. nov., *Zobellia laminariae* sp. nov. and *Zobellia russellii* sp. nov., novel marine bacteria of the family *Flavobacteriaceae*. Int J Syst Evol Microbiol. 2004;54(5):1643–8.

38. Nedashkovskaya O, Otstavnykh N, Zhukova N, Guzev K, Chausova V, Tekutyeva L, et al. *Zobellia barbeyronii* sp. nov., a new member of the family *Flavobacteriaceae*, isolated from seaweed, and emended description of the species *Z. amurskyensis*, *Z. laminariae*, *Z. russellii* and *Z. uliginosa*. Diversity. 2021;13(11):520.

39. Barbeyron T, Thomas F, Barbe V, Teeling H, Schenowitz C, Dossat C, et al. Habitat and taxon as driving forces of carbohydrate catabolism in marine heterotrophic bacteria: Example of the model algae-associated bacterium *Zobellia galactanivorans* Dsij^{T}. Environ Microbiol. 2016;18:4610–27.

40. Chernysheva N, Bystritskaya E, Stenkova A, Golovkin I. Comparative genomics and CAZyme genome repertoires of marine *Zobellia amurskyensis* KMM 3526^{T} and *Zobellia laminariae* KMM 3676^{T}. 2019;17(12):661.

41. Chernysheva N, Bystritskaya E, Likhatskaya G, Nedashkovskaya O, Isaeva M. Genome-wide analysis of PL7 alginate lyases in the genus *Zobellia*. Molecules. 2021;26(8):2387.

42. Potin P, Sanseau A, Le Gall Y, Rochas C, Kloareg B. Purification and characterization of a new k□carrageenase from a marine *Cytophaga*□like bacterium. Eur J Biochem. 1991;201(1):241–7.

43. Lami R, Grimaud R, Sanchez-Brosseau S, Six C, Thomas F, West NJ, et al. Marine

bacterial models for experimental biology. In: Boutet A, Schierwater B, editors. Handbook of Marine Model Organisms in Experimental Biology. 2021.

44. Dudek M, Dieudonné A, Jouanneau D, Rochat T, Michel G, Sarels B, et al. Regulation of alginate catabolism involves a GntR family repressor in the marine flavobacterium *Zobellia galactanivorans* Dsij^{T}. Nucleic Acids Res. 2020;48(14):7786–800.

45. Thomas F, Lundqvist LCE, Jam M, Jeudy A, Barbeyron T, Sandström C, et al. Comparative characterization of two marine alginate lyases from *Zobellia galactanivorans* reveals distinct modes of action and exquisite adaptation to their natural substrate. J Biol Chem. 2013;288(32):23021–37.

46. Thomas F, Barbeyron T, Tonon T, Génicot S, Czjzek M, Michel G. Characterization of the first alginolytic operons in a marine bacterium: from their emergence in marine *Flavobacteriia* to their independent transfers to marine *Proteobacteria* and human gut *Bacteroides*. Environ Microbiol. 2012;14(9):2379–94.

47. Jam M, Flament D, Allouch J, Potin P, Thion L, Kloareg B, et al. The endo-β-agarases AgaA and AgaB from the marine bacterium *Zobellia galactanivorans*: Two paralogue enzymes with different molecular organizations and catalytic behaviours. Biochem J. 2005;385(3):703–13.

48. Hehemann JH, Correc G, Thomas F, Bernard T, Barbeyron T, Jam M, et al. Biochemical and structural characterization of the complex agarolytic enzyme system from the marine bacterium *Zobellia galactanivorans*. J Biol Chem. 2012;287(36):30571–84.

49. Labourel A, Jam M, Jeudy A, Hehemann JH, Czjzek M, Michel G. The β-glucanase ZgLamA from *Zobellia galactanivorans* evolved a bent active site adapted for efficient

627 degradation of algal laminarin. J Biol Chem. 2014;289(4):2027–42.

628 50. Labourel A, Jam M, Legentil L, Sylla B, Hehemann JH, Ferrières V, et al. Structural
629 and biochemical characterization of the laminarinase ZgLamCGH16 from *Zobellia*
630 *galactanivorans* suggests preferred recognition of branched laminarin. Acta
631 Crystallogr. 2015;D71:173–84.

632 51. Dorival J, Ruppert S, Gunnoo M, Orłowski A, Chapelais-Baron M, Dabin J, et al. The
633 laterally-acquired GH5 ZgEngAGH5_4 from the marine bacterium *Zobellia*
634 *galactanivorans* is dedicated to hemicellulose hydrolysis. Biochem J.
635 2018;475(22):3609–28.

636 52. Groisillier A, Labourel A, Michel G, Tonon T. The mannitol utilization system of the
637 marine bacterium *Zobellia galactanivorans*. Appl Environ Microbiol.
638 2015;81(5):1799–812.

639 53. Fournier JB, Rebuffet E, Delage L, Grijol R, Meslet-Cladière L, Rzonca J, et al. The
640 vanadium iodoperoxidase from the marine *Flavobacteriaceae* species *Zobellia*
641 *galactanivorans* reveals novel molecular and evolutionary features of halide specificity
642 in the vanadium haloperoxidase enzyme family. Appl Environ Microbiol.
643 2014;80(24):7561–73.

644 54. Grigorian E, Groisillier A, Thomas F, Leblanc C, Delage L. Functional characterization
645 of a L-2-haloacid dehalogenase from *Zobellia galactanivorans* Dsij^{T} suggests a role in
646 haloacetic acid catabolism and a wide distribution in marine environments. Front
647 Microbiol. 2021;12:725997.

648 55. Zhu Y, Thomas F, Larocque R, Li N, Duffieux D, Cladière L, et al. Genetic analyses
649 unravel the crucial role of a horizontally acquired alginate lyase for brown algal

biomass degradation by *Zobellia galactanivorans*. Environ Microbiol. 2017;19(6):2164–81.

56. Zablackis E, Perez J. A partially pyruvated carrageenan from hawaiian *Grateloupia filicina* (Cryptonemiales, Rhodophyta). Bot Mar. 1990;33(3):273–6.

57. Filisetti-Cozzi T, Carpita N. Measurement of uronic acids without interference from neutral sugars. Anal Biochem. 1991;197(1):15162.

58. Blumenkrantz N, Asboe-Hansen G. New method for quantitative determination of uronic acids. Anal Biochem. 1973;54(2):484–9.

59. Cumashi A, Ushakova NA, Preobrazhenskaya ME, D'Incecco A, Piccoli A, Totani L, et al. A comparative study of the anti-inflammatory, anticoagulant, antiangiogenic, and antiadhesive activities of nine different fucoidans from brown seaweeds. Glycobiology. 2007;17(5):541–52.

60. ZoBell C. Studies on marine bacteria. I. The cultural requirements of heterotrophic aerobes. J Mar Res. 1941;4:75.

61. Klindworth A, Pruesse E, Schweer T, Peplies J, Quast C, Horn M, et al. Evaluation of general 16S ribosomal RNA gene PCR primers for classical and next-generation sequencing-based diversity studies. Nucleic Acids Res. 2013;41(1):e1.

62. Patro R, Duggal G, Love MI, Irizarry RA, Kingsford C. Salmon provides fast and bias-aware quantification of transcript expression. Nat Methods. 2017;14(4):417–9.

63. Love MI, Huber W, Anders S. Moderated estimation of fold change and dispersion for RNA-seq data with DESeq2. Genome Biol. 2014;15(12):1–21.

64. R Core Team. R: A language and environment for statistical computing. Vienna,

Austria: R Foundation for Statistical Computing; 2018.

65. Lex A, Gehlenborg N, Strobelt H. UpSet: Visualization of intersecting sets. IEEE Trans Vis Comput Graph. 2014;20(12):1983–92.

66. Krassowski M. krassowski/complex-upset. 2020.

67. Murtagh F, Legendre P. Ward's hierarchical clustering method: clustering criterion and agglomerative algorithm. J Classif. 2014;31:274–95.

68. Wickham H. Use R! ggplot2: Elegant graphics for data analysis. Second Edition. 2016.

69. Kidby DK, Davidson DJ. Ferricyanide estimation of sugars in the nanomole range. Anal Biochem. 1973;55:321–5.

70. Zhang H, Yohe T, Huang L, Entwistle S, Wu P, Yang Z, et al. DbCAN2: A meta server for automated carbohydrate-active enzyme annotation. Nucleic Acids Res. 2018;46(W1):W95–101.

71. Chen X, Hu Y, Yang B, Gong X, Zhang N, Niu L, et al. Structure of lpg0406, a carboxymuconolactone decarboxylase family protein possibly involved in antioxidative response from *Legionella pneumophila*. Protein Sci. 2015;24(12):2070–5.

72. Handa N, Terada T, Doi-katayama Y, HIrota H, Tame J, Park A, et al. Crystal structure of a novel polyisoprenoid-binding protein from *Thermus thermophilus* HB8. Protein Sci. 2005;14(4):1004–10.

73. Weber A, Kögl SA, Jung K. Time-dependent proteome alterations under osmotic stress during aerobic and anaerobic growth in *Escherichia coli*. J Bacteriol. 2006;188(20):7165–75.

74. Enke TN, Datta MS, Schwartzman J, Cermak N, Schmitz D, Barrere J, et al. Modular

694 assembly of polysaccharide-degrading marine microbial communities. Curr Biol.
695 2019;29(9):1528-1535.e6.

696 75. Pollak S, Gralka M, Sato Y, Schwartzman J, Lu L, Cordero OX. Public good
697 exploitation in natural bacterioplankton communities. Sci Adv. 2021;7:eabi4717.

698 76. Pontrelli S, Szabo R, Pollak S, Schwartzman J, Ledezma D, Cordero OX, et al.
699 Hierarchical control of microbial community assembly. bioRxiv [Internet]. 2021;
700 Available from: https://doi.org/10.1101/2021.06.22.449372

701 77. Holdt SL, Kraan S. Bioactive compounds in seaweed: Functional food applications and
702 legislation. J Appl Phycol. 2011;23(3):543–97.

703 78. Kawamura-Konishi Y, Watanabe N, Saito M, Nakajima N, Sakaki T, Katayama T, et
704 al. Isolation of a new phlorotannin, a potent inhibitor of carbohydrate-hydrolyzing
705 enzymes, from the brown alga *Sargassum patens*. J Agric Food Chem.
706 2012;60(22):5565–70.

707 79. Garbary DJ, Brown NE, MacDonell HJ, Toxopeux J. *Ascophyllum* and its symbionts
708 — A complex symbiotic community on North Atlantic shores. In: Algal and
709 Cyanobacteria Symbioses. 2017. p. 547–72.

710 80. Pluvinage B, Grondin JM, Amundsen C, Klassen L, Moote PE, Xiao Y, et al.
711 Molecular basis of an agarose metabolic pathway acquired by a human intestinal
712 symbiont. Nat Commun. 2018;9:1043.

713 81. Reintjes G, Arnosti C, Fuchs BM, Amann R. An alternative polysaccharide uptake
714 mechanism of marine bacteria. ISME J. 2017;11(7):1640–50.

715 82. Mabeau S, Kloareg B, Joseleau J-P. Fractionation and analysis of fucans from brown

algae. Phytochemistry. 1990;29(8):2441–5.

83. Küpper FC, Kloareg B, Guern J, Potin P. Oligoguluronates elicit an oxidative burst in the brown algal kelp *Laminaria digitata*. Plant Physiol. 2001;125(1):278–91.

84. Küpper FC, Müller DG, Peters AF, Kloareg B, Potin P. Oligoalginate recognition and oxidative burst play a key role in natural and induced resistance of sporophytes of *Laminariales*. Ann Oper Res. 2002;28(10):2057–81.

85. Sato K, Naito M, Yukitake H, Hirakawa H, Shoji M, McBride MJ, et al. A protein secretion system linked to bacteroidete gliding motility and pathogenesis. PNAS. 2010;107(1):276–81.

86. Eckroat TJ, Greguske C, Hunnicutt DW. The type 9 secretion system is required for *Flavobacterium johnsoniae* biofilm formation. Front Microbiol. 2021;12:660887.

87. Xie S, Tan Y, Song W, Zhang W, Qi Q, Lu X. N-glycosylation of a cargo protein C-terminal domain recognized by the type IX secretion system in *Cytophaga hutchinsonii* affects protein secretion and localization. Appl Environ Microbiol. 2021.

Figure legends

Figure 1: Ability of *Z. galactanivorans* Dsij^T to use fresh brown macroalgae for its growth. (A) Growth of *Z. galactanivorans* with either macroalgae pieces (*Laminaria digitata*, *Fucus serratus* and *Ascophyllum nodosum*) or purified sugars (maltose, alginate and FCSPs). Individual points for replicate experiments are shown. Lines are means of independent replicates (n = 2 or n = 3). (B) Photographs showing the integrity of the *L. digitata* tissues after 65 h. (C) *L. digitata* tissues colonization by *Z. galactanivorans* during the degradation. Micrographs are overlay of the CARD–FISH signal (magenta, *Zobellia*-specific probe with Alexa488 as the reporter signal) and the algal autofluorescence (green) and were obtained with the surface channel mode of the 3D viewer. For the different times, transversal views are shown on the left and top views on the right. The non-fluorescent gap between the bacterial cells and the algal cells likely represent the mucilage coat of *L. digitata*. The absence of algal autofluorescence signal below 25-30 µm is the result of its rapid decrease in intensity as we move away from the coverslip.

Figure 2: General features of the transcriptomic responses occurring in free-living *Z. galactanivorans* Dsij^T during growth with macroalgae. (A) Principal Component Analysis of the gene expression. (B) Upset plot of the differentially expressed genes with maltose as the control condition (Bonferroni-adjusted p-value < 0.05 and |log2FC| > 2). Set size represents the total amount of genes regulated in each condition.

Figure 3: Regulation of the catabolic pathways during the degradation of fresh algal tissues. (A) Heatmap of the 51 PULs identified in the genome of *Z. galactanivorans* Dsij^T. PUL 1 to 50 were identified during the annotation of the *Z. galactanivorans* Dsij^T genome by the presence of the susCD-like pair (Supplementary Table S3 in (39)). PUL51 targeting 3,6-anhydro-D-galactose and involved in carrageenan catabolism (but lacking the susCD-like

pair) was further described (25). For each PUL, the mean log2FC of all genes is represented, taking maltose as a control condition. Carbon sources and PULs were arranged according to a hierarchical clustering analysis (Ward's method). A PUL was considered regulated (induced in red, repressed in blue) if more than 50 % of the genes were significantly differentially expressed (*) and strongly regulated if more than 80 % of the genes were significantly differentially expressed (**). Putative substrates targeted by the PULs are indicated. Hash signs denote PULs biochemically characterized previously in *Z. galactanivorans* (##) or in another organism (#). (B) Heatmap representing the log2FC of individual genes contained in the PULs induced with macroalgae and which clustered together in A. (C) Activity of extracellular polysaccharidases secreted in the microcosms containing macroalgae. The mean value measured in the uninoculated controls was subtracted from each value. Bars are means of independent replicates (n = 2 or 3) shown as individual points. Significant difference from zero was tested when n = 3 (t-test; *, P<0.05). *L. dig*: *Laminaria digitata*; *F. ser*: *Fucus serratus*; *A. nod*: *Ascophyllum nodosum*; FCSP: fucose containing sulfated polysaccharide; PS: Polysaccharide.

Figure 4: Selection of genes specifically induced by fresh macroalgae. Mean expression values (n = 3, except for *F. serratus* n = 2) of selected genes significantly triggered (*) with at least one macroalgae compared to both the purified polysaccharides and maltose (see SuppTable 4). No dot was represented if the mean read count was below 200. *L. dig*: *Laminaria digitata*; *F. ser*: *Fucus serratus*; *A. nod*: *Ascophyllum nodosum*; Malt.: Maltose; Algi.: Alginate; FCSP: fucose containing sulfated polysaccharide

Figure 5: Effect of the attachment to macroalgae during the degradation. (A) Number of genes (Bonferroni-adjusted p-value < 0.05) up-regulated in algae-attached bacteria compared

782 to free-living bacteria. The annotation of each gene is provided. (B) Alginolytic activity of the
783 enzymes secreted when *Z. galactanivorans* was grown in contact with *L. digitata* (black) or
784 separated from *L. digitata* by a 0.2 µm filter (red). The activity was measured in each
785 compartment (left and right) and summed. Values are mean ± s.d. (n = 3).

786

787 **Figure 6: Ability of *Zobellia* spp. to use fresh *L. digitata* for its growth.** (A) Growth of
788 eight *Zobellia* strains with *L. digitata* pieces (meristem of adult individuals). The generation
789 time t_{gen} is indicated for each strain as well as the number of glycoside hydrolases (GH, blue),
790 polysaccharides lyases (PL, yellow), carbohydrate esterases (CE, orange) and sulfatases (S,
791 red) predicted in their genome (dbCAN search on the MaGe platform). Individual points for
792 duplicate experiments are shown. Lines are means of independent replicates (n = 2 or n = 3).
793 (B) Comparison of genomic loci among the eight *Zobellia* strains. For *Z. galactanivorans,*
794 genes were colored according to their expression log2FC for the comparison *L. digitata* vs.
795 maltose. Gene ID is indicated inside arrows and CAZymes and sulfatases are specified above.
796 Top: genes involved in the alginate-utilization system. Bottom: genes contained in putative
797 FCSP PUL34 and 35. Zgal: *Z. galactanivorans* Dsij^T; Zamu: *Z. amurskyensis* KMM 3526^T;
798 Zlam: *Z. laminariae* KMM 3676^T; Zrus: *Z. russellii* KMM 3677^T; ZrosF08: *Z. roscoffensis*
799 Asnod1-F08^T; ZrosB02: *Z. roscoffensis* Asnod2-B02-B; ZnedB07: *Z. nedashkovskayae*
800 Asnod2-B07-B^T; ZnedE08: *Z. nedashkovskayae* Asnod3-E08-A.
801

A

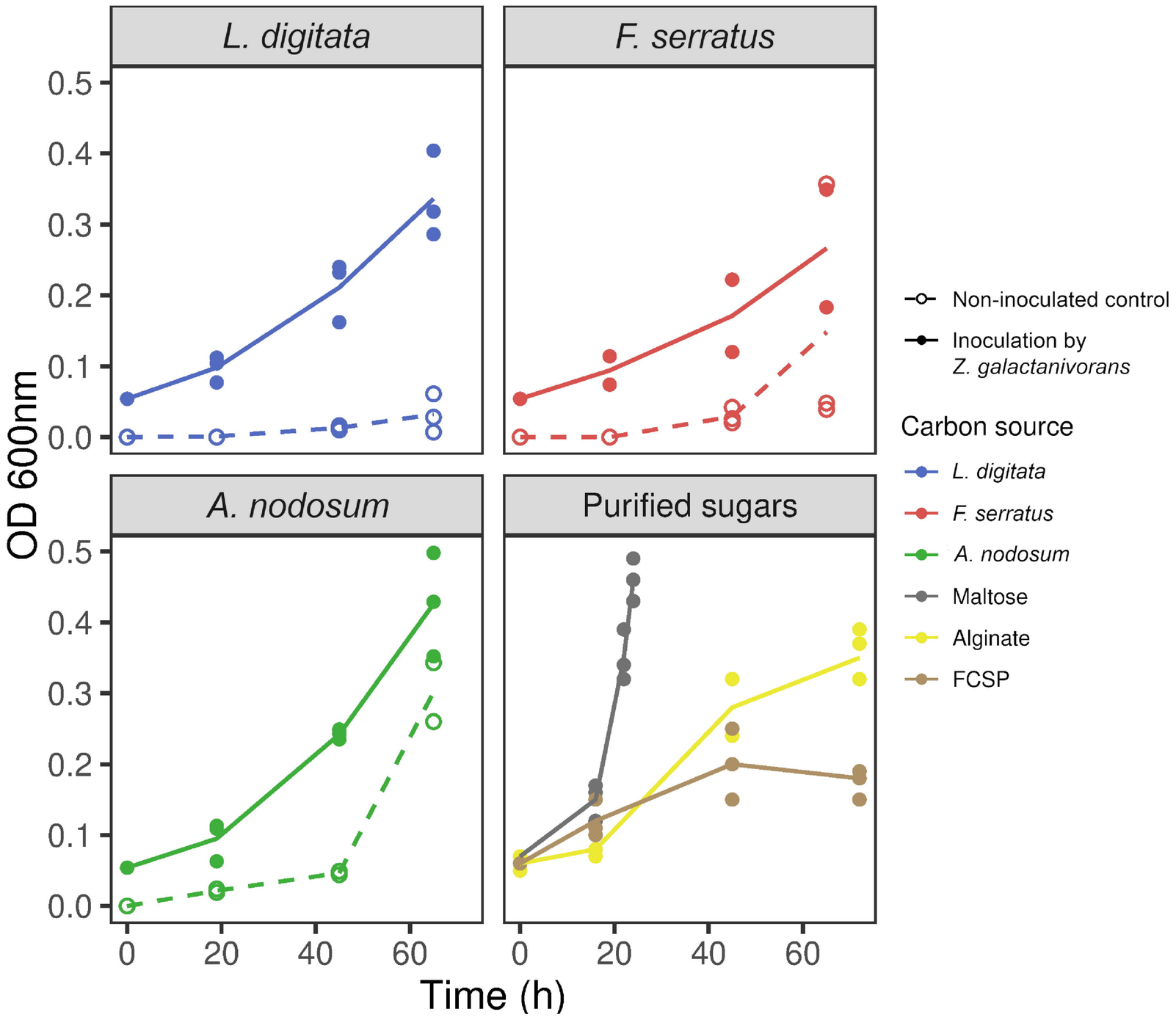

B

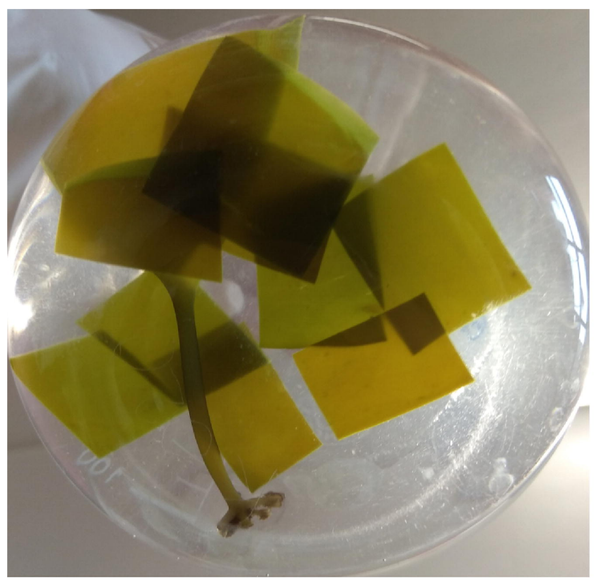

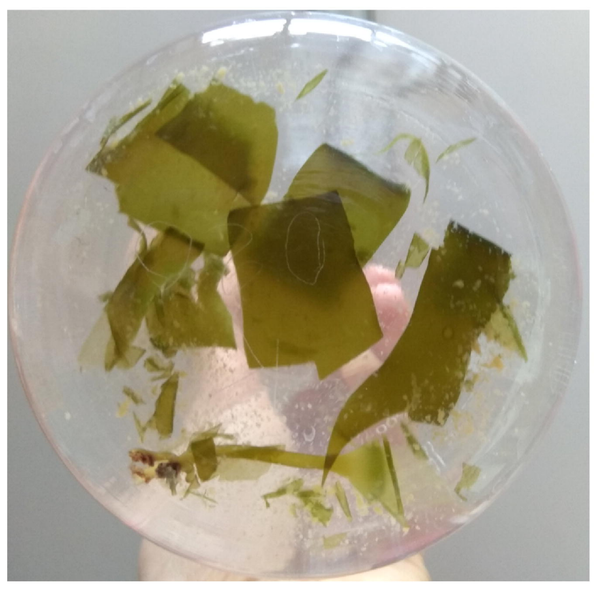

C

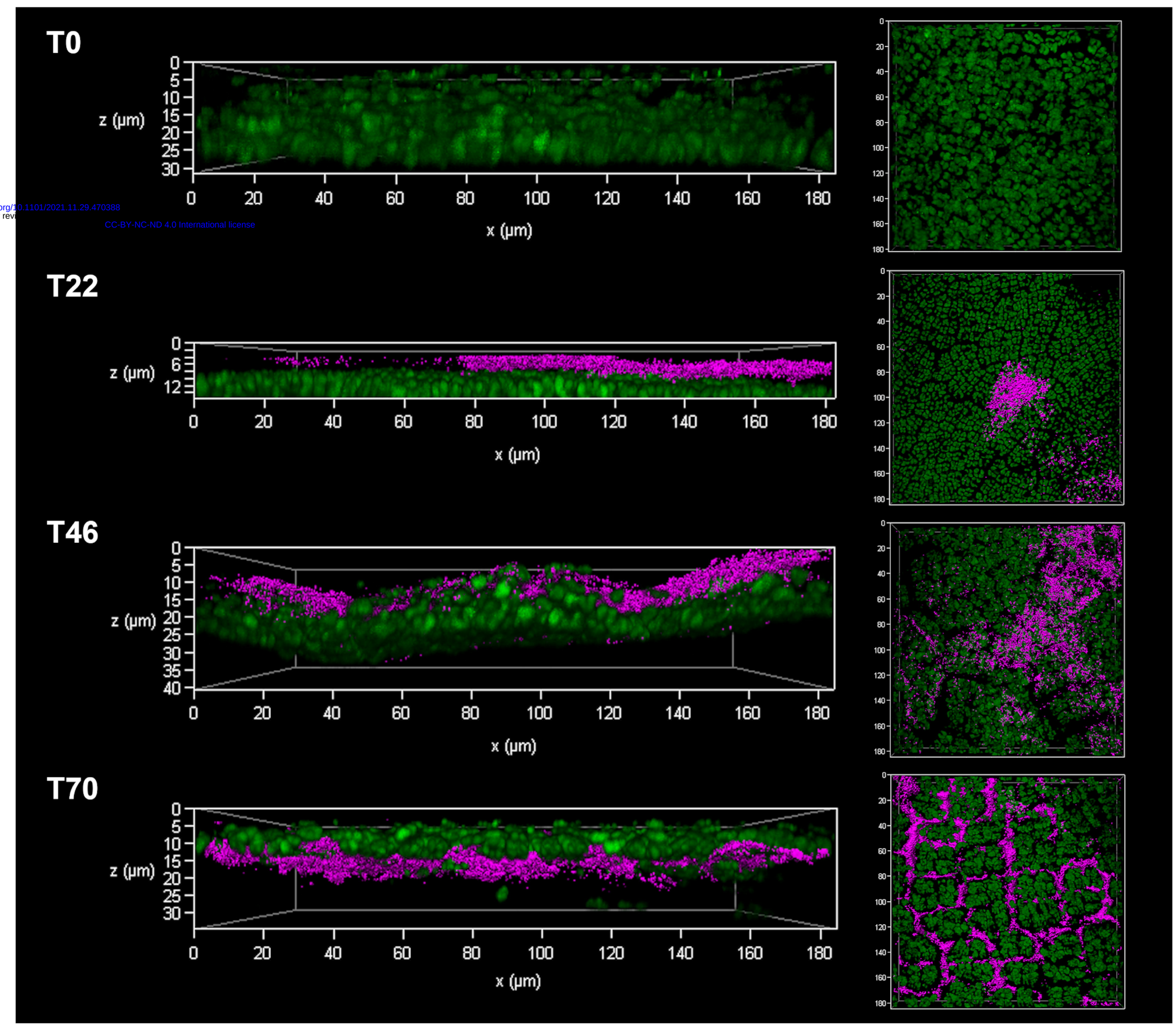

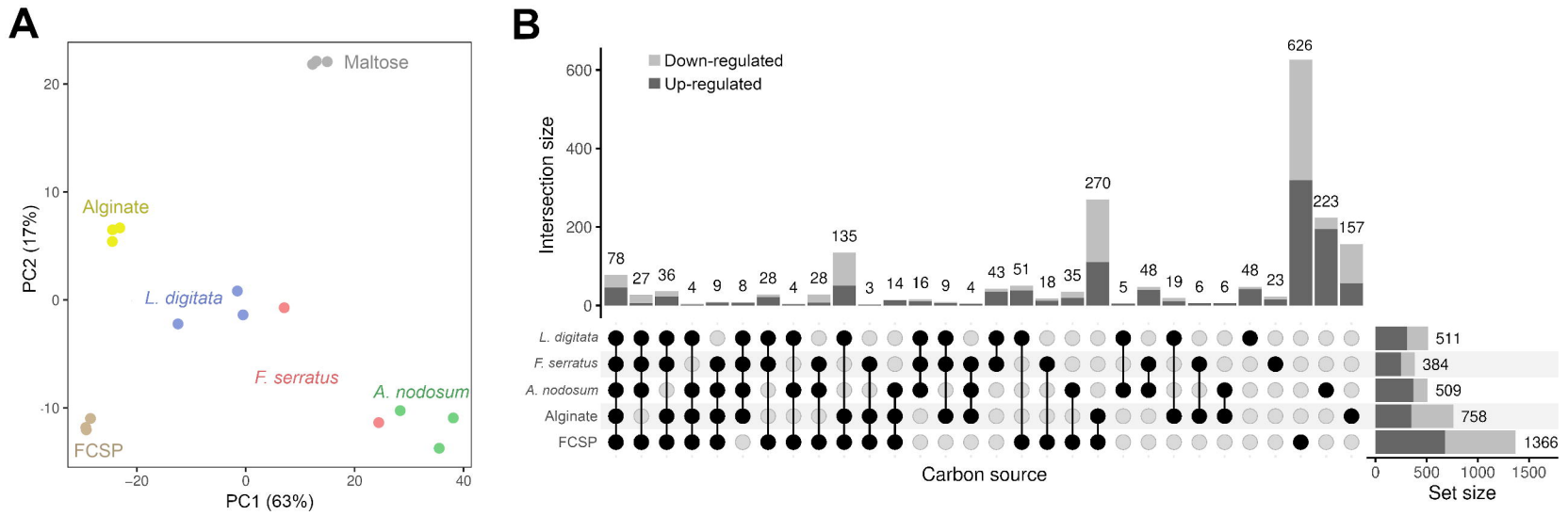
A
Maltose
Alginate
L. digitata
F. serratus
A. nodosum
FCSP
PC2 (17%)
PC1 (63%)
20
10
0
-10
-20
0
20
40
B
Down-regulated
Up-regulated
Intersection size
600
400
200
0
78
27
36
4
9
8
28
4
28
135
3
14
16
9
4
43
51
18
35
270
5
48
19
6
6
48
23
626
223
157
L. digitata
F. serratus
A. nodosum
Alginate
FCSP
511
384
509
758
1366
Carbon source
0
500
1000
1500
Set size

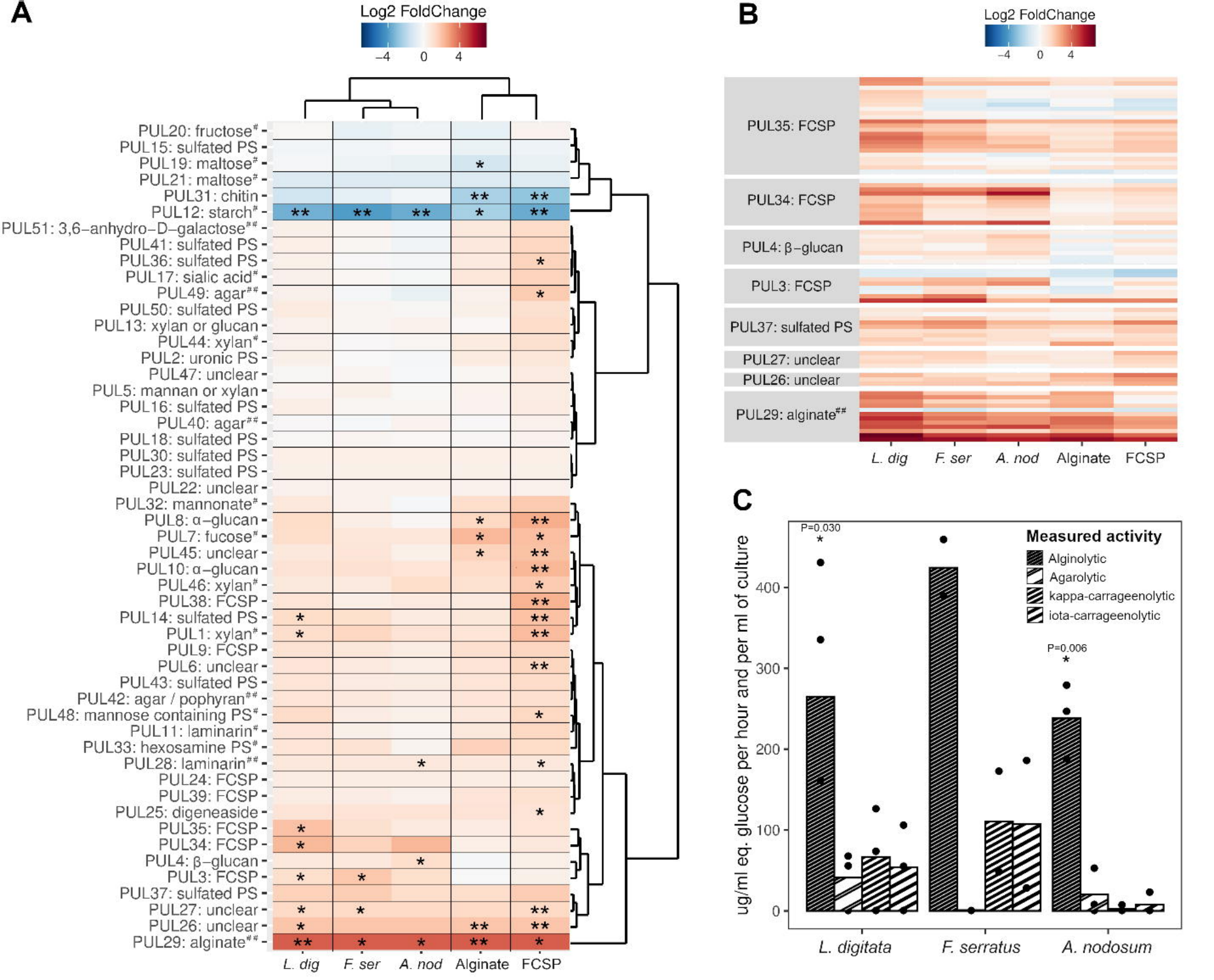
A
Log2 FoldChange
−4
0
4
PUL20: fructose#
PUL15: sulfated PS
PUL19: maltose#
PUL21: maltose#
PUL31: chitin
PUL12: starch#
PUL51: 3,6−anhydro−D−galactose##
PUL41: sulfated PS
PUL36: sulfated PS
PUL17: sialic acid#
PUL49: agar##
PUL50: sulfated PS
PUL13: xylan or glucan
PUL44: xylan#
PUL2: uronic PS
PUL47: unclear
PUL5: mannan or xylan
PUL16: sulfated PS
PUL40: agar##
PUL18: sulfated PS
PUL30: sulfated PS
PUL23: sulfated PS
PUL22: unclear
PUL32: mannonate#
PUL8: α−glucan
PUL7: fucose#
PUL45: unclear
PUL10: α−glucan
PUL46: xylan#
PUL38: FCSP
PUL14: sulfated PS
PUL1: xylan#
PUL9: FCSP
PUL6: unclear
PUL43: sulfated PS
PUL42: agar / pophyran##
PUL48: mannose containing PS#
PUL11: laminarin#
PUL33: hexosamine PS#
PUL28: laminarin##
PUL24: FCSP
PUL39: FCSP
PUL25: digeneaside
PUL35: FCSP
PUL34: FCSP
PUL4: β−glucan
PUL3: FCSP
PUL37: sulfated PS
PUL27: unclear
PUL26: unclear
PUL29: alginate##
L. dig
F. ser
A. nod
Alginate
FCSP
B
Log2 FoldChange
−4
0
4
PUL35: FCSP
PUL34: FCSP
PUL4: β−glucan
PUL3: FCSP
PUL37: sulfated PS
PUL27: unclear
PUL26: unclear
PUL29: alginate##
L. dig
F. ser
A. nod
Alginate
FCSP
C
P=0.030
P=0.006
Measured activity
Alginolytic
Agarolytic
kappa-carrageenolytic
iota-carrageenolytic
ug/ml eq. glucose per hour and per ml of culture
0
100
200
300
400
L. digitata
F. serratus
A. nodosum

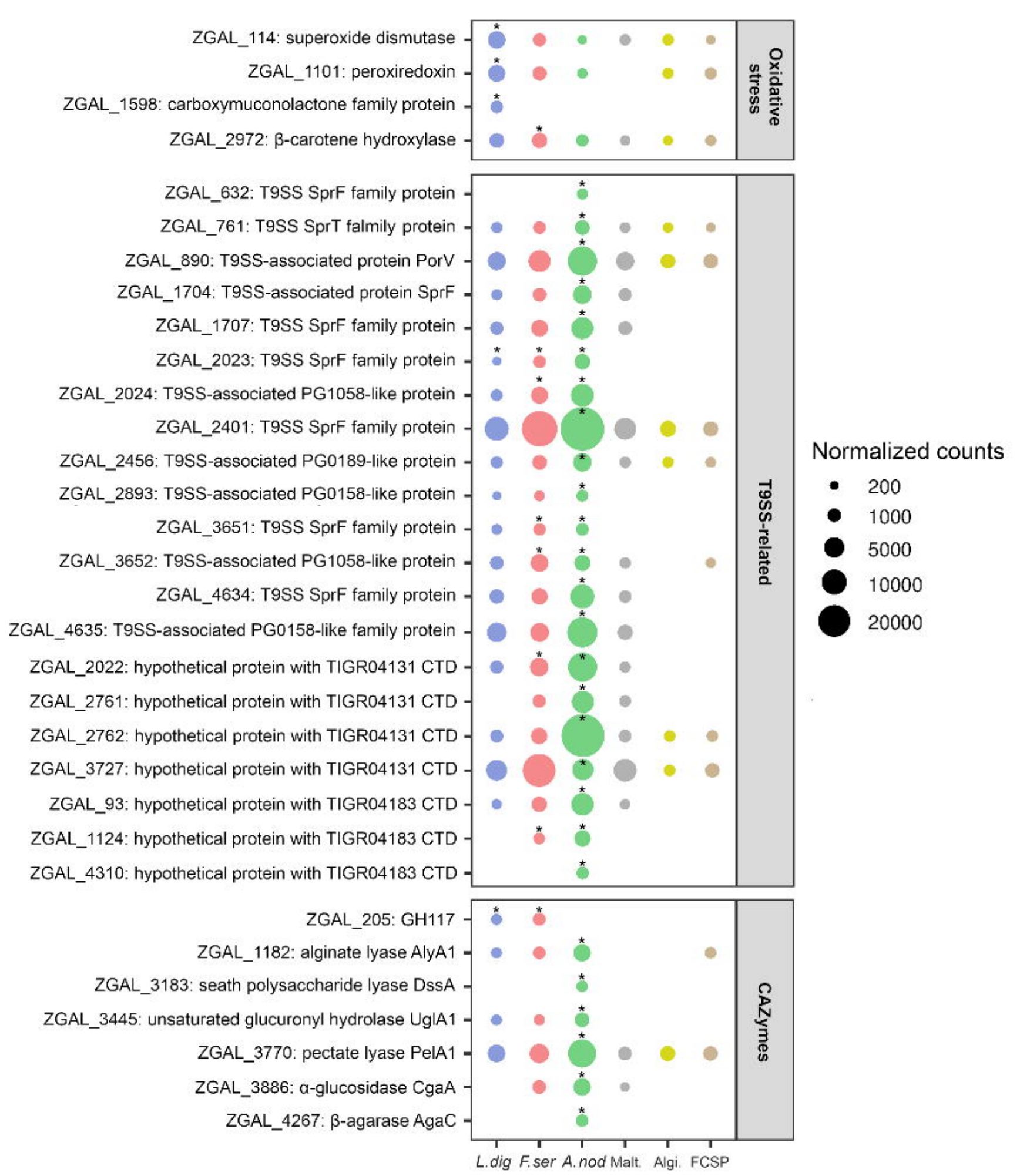
ZGAL_114: superoxide dismutase
ZGAL_1101: peroxiredoxin
ZGAL_1598: carboxymuconolactone family protein
ZGAL_2972: β-carotene hydroxylase
Oxidative stress
ZGAL_632: T9SS SprF family protein
ZGAL_761: T9SS SprT falmily protein
ZGAL_890: T9SS-associated protein PorV
ZGAL_1704: T9SS-associated protein SprF
ZGAL_1707: T9SS SprF family protein
ZGAL_2023: T9SS SprF family protein
ZGAL_2024: T9SS-associated PG1058-like protein
ZGAL_2401: T9SS SprF family protein
ZGAL_2456: T9SS-associated PG0189-like protein
ZGAL_2893: T9SS-associated PG0158-like protein
ZGAL_3651: T9SS SprF family protein
ZGAL_3652: T9SS-associated PG1058-like protein
ZGAL_4634: T9SS SprF family protein
ZGAL_4635: T9SS-associated PG0158-like family protein
ZGAL_2022: hypothetical protein with TIGR04131 CTD
ZGAL_2761: hypothetical protein with TIGR04131 CTD
ZGAL_2762: hypothetical protein with TIGR04131 CTD
ZGAL_3727: hypothetical protein with TIGR04131 CTD
ZGAL_93: hypothetical protein with TIGR04183 CTD
ZGAL_1124: hypothetical protein with TIGR04183 CTD
ZGAL_4310: hypothetical protein with TIGR04183 CTD
T9SS-related
ZGAL_205: GH117
ZGAL_1182: alginate lyase AlyA1
ZGAL_3183: seath polysaccharide lyase DssA
ZGAL_3445: unsaturated glucuronyl hydrolase UglA1
ZGAL_3770: pectate lyase PelA1
ZGAL_3886: α-glucosidase CgaA
ZGAL_4267: β-agarase AgaC
CAZymes
L.dig
F.ser
A.nod
Malt.
Algi.
FCSP
Normalized counts
200
1000
5000
10000
20000

A

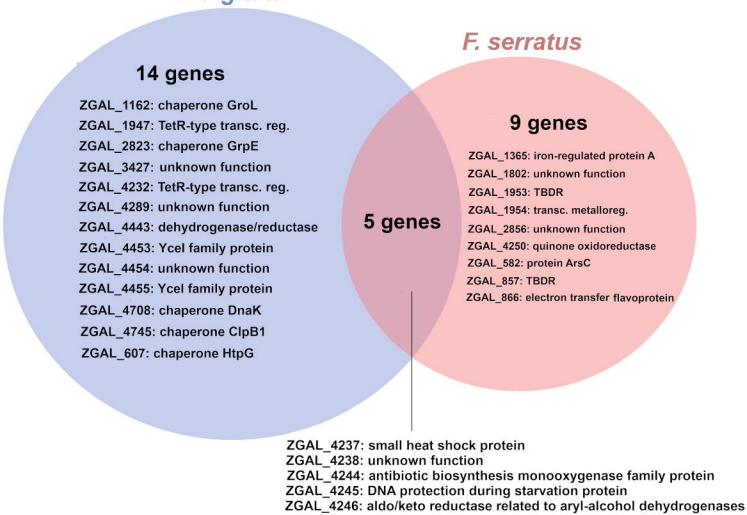
L. digitata
F. serratus
14 genes
ZGAL_1162: chaperone GroL
ZGAL_1947: TetR-type transc. reg.
ZGAL_2823: chaperone GrpE
ZGAL_3427: unknown function
ZGAL_4232: TetR-type transc. reg.
ZGAL_4289: unknown function
ZGAL_4443: dehydrogenase/reductase
ZGAL_4453: YceI family protein
ZGAL_4454: unknown function
ZGAL_4455: YceI family protein
ZGAL_4708: chaperone DnaK
ZGAL_4745: chaperone ClpB1
ZGAL_607: chaperone HtpG
5 genes
9 genes
ZGAL_1365: iron-regulated protein A
ZGAL_1802: unknown function
ZGAL_1953: TBDR
ZGAL_1954: transc. metalloreg.
ZGAL_2856: unknown function
ZGAL_4250: quinone oxidoreductase
ZGAL_582: protein ArsC
ZGAL_857: TBDR
ZGAL_866: electron transfer flavoprotein
ZGAL_4237: small heat shock protein
ZGAL_4238: unknown function
ZGAL_4244: antibiotic biosynthesis monooxygenase family protein
ZGAL_4245: DNA protection during starvation protein
ZGAL_4246: aldo/keto reductase related to aryl-alcohol dehydrogenases

B

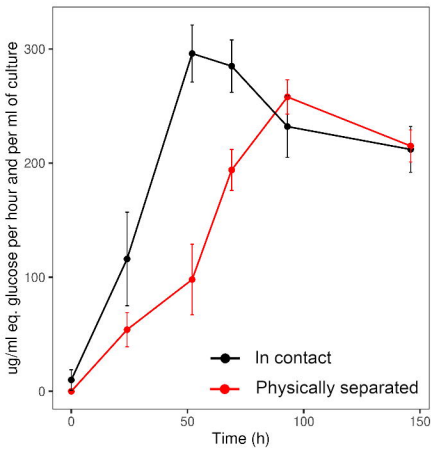
ug/ml eq. glucose per hour and per ml of culture
300
200
100
0
0
50
100
150
Time (h)
In contact
Physically separated

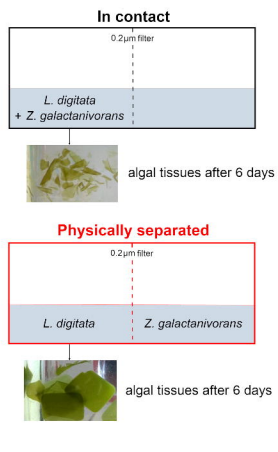
In contact
0.2µm filter
L. digitata
+ Z. galactanivorans
algal tissues after 6 days
Physically separated
0.2µm filter
L. digitata
Z. galactanivorans
algal tissues after 6 days

A

Z. galactanivorans Dsij^T

Z. amurskyensis KMM3526^T

Z. laminariae KMM3676^T

Z. russellii KMM3677^T

Z. roscoffensis Asnod1-F08^T

Z. roscoffensis Asnod2-B02-B

Z. nedashkovskayae Asnod2-B07-B^T

Z. nedashkovskayae Asnod3-E08-A

Non-inoculated control

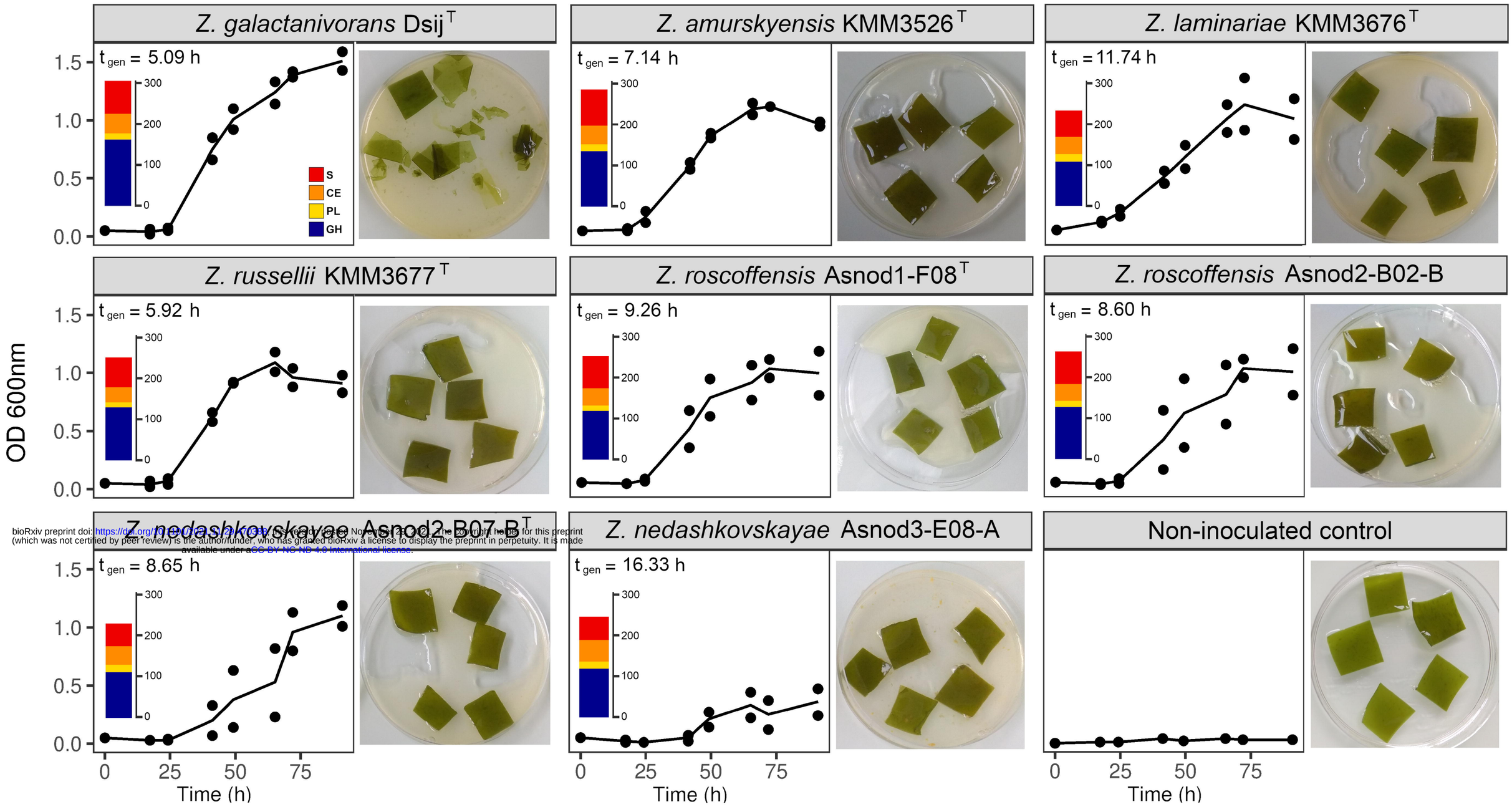

B